

# Dual-Frequency and Dual-Polarization Microstrip Antennas for SAR Applications

Ralph Pokuls, Jaroslaw Uher, *Member, IEEE*, and D. M. Pozar, *Fellow, IEEE*

**Abstract**— This paper discusses various methods of implementing a shared-aperture dual-frequency dual-polarized array antenna for space-based synthetic aperture radar (SAR) applications. After evaluating the use of several potential array architecture concepts and radiating elements, a design using interlaced *C*-band microstrip patches and *X*-band printed slot elements was chosen as the best choice for the present system requirements. Layout considerations for the two arrays and their associated feed networks are addressed in terms of a practical design. A dual-frequency (*C*- and *X*-band), dual-linear polarized SAR array antenna prototype was designed, fabricated, and tested. The principal goal of this effort was to demonstrate the viability of the dual-band dual-polarized array concept, and this has been accomplished. Test results are shown with good correlation between measured and predicted results, validating the design approach used. This work demonstrates that a dual-frequency dual-polarization SAR antenna within a single aperture is a feasible approach to meeting user requirements in future SAR spacecraft.

**Index Terms**— Microstrip antennas, synthetic aperture radar.

## I. INTRODUCTION

FUTURE requirements for advanced SAR antennas include the need for dual-frequency operation using a single aperture. It is also desirable that the dual-frequency antenna will be simultaneously capable of dual-polarization operation. Two frequencies (*L*-band and *C*-band) and dual polarization were used for the shuttle imaging radar (SIR-C) mission [1], [2], but the *L*-band and *C*-band antenna did not share a common aperture. As a consequence, the SIR-C antenna mass was large (795-kg *L*-band and 370-kg *C*-band) and would not be compatible with currently operated space platforms. In practice, only a single aperture antenna has the capability of integration with a spacecraft of minimum size and cost.

The work described in this paper focuses on the design of a *C*-band and *X*-band dual-linear polarized synthetic aperture radar (SAR) antenna sharing the same physical aperture. SAR systems requirements place strong demands on the performance of the antenna and it is these requirements that must be considered when choosing a design approach. This study examines alternative design approaches for a dual-frequency dual-polarized (DFDP) antenna and develops radiating element designs to enable a proof-of-concept antenna to be built and tested. The performance of this array was evaluated and

compared with theoretical model predictions created with commercial software, demonstrating close correlation between predictions and measured results and showing that the DFDP concept is viable for development and can meet the full requirements of spaceborne SAR applications.

The paper is organized into eight sections. In Section II, the basic performance requirements for the DFDP antenna are reviewed. Section III deals with a tradeoff study of candidate dual-frequency radiating elements that are suitable for SAR application. Section IV provides details on the radiating element design and Section V describes the overall design approach for the proof-of-concept antenna. Section VI includes the proof-of-concept antenna description, Section VII provides a measured antenna performance, and conclusions are given in Section VIII.

## II. DUAL-FREQUENCY DUAL-POLARIZATION ANTENNA REQUIREMENTS

For space-based SAR systems the most significant element in determining overall system performance is the antenna. Its capability has major impact on system sensitivity, spatial resolution in both range and azimuth, image ambiguities, and swath coverage. The majority of these aspects are primarily influenced by the beam forming and beam scanning capability of the antenna, which must be optimized within the volume and mass constraints inherent in the space environment. With the exception of the *L*-, *C*-, and *X*-band SIR-C short-duration Shuttle mission, space-based SAR's have (to date) been single-frequency single-polarization instruments, providing what is in effect a monochrome image. SIR-C and airborne instruments have demonstrated that the utility and, therefore, value of the data is considerably enhanced by adding dual polarization and a second frequency. Generally, high frequencies result in energy being reflected from the surface, providing an almost optical quality to the image with low frequencies achieving some penetration to give information relating to bulk properties. Polarization has a strong influence on reflectivity where the scene being imaged has a clear correlation to the structure, such as occurs with the trunks of trees or ocean waves.

For the development reported in this paper, frequencies of 5.3 GHz (*C*-band) and 9.6 GHz (*X*-band) were selected with a requirement that the concepts developed should be transformable to other pairs of frequency bands. Using high frequencies was expected to be more demanding in terms of design and enabled a physically smaller test unit to be built.

Manuscript received July 31, 1996; revised March 25, 1998.

R. Pokuls and J. Uher are with Spar Aerospace Ltd., Montreal, H9X 3R2 Canada.

D. M. Pozar is with the ECE Department, University of Massachusetts, Amherst, MA 01003 USA.

Publisher Item Identifier S 0018-926X(98)06872-0.

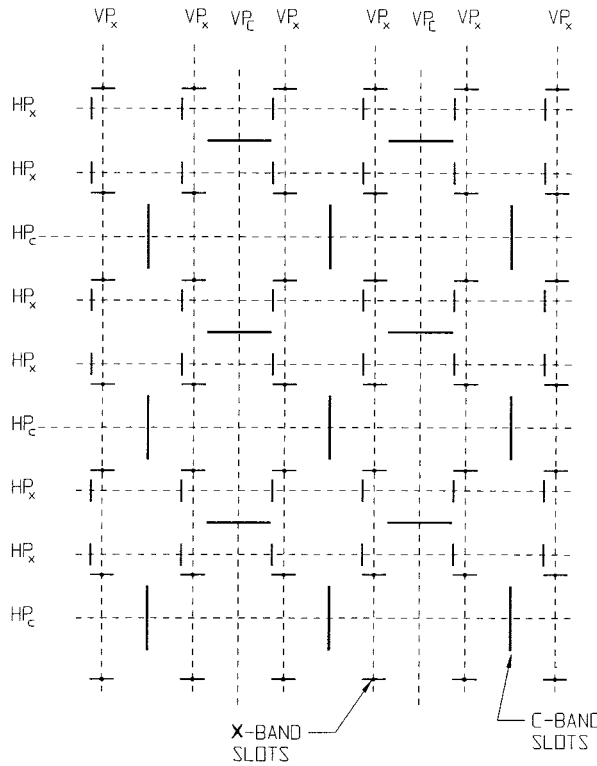


Fig. 1. Dual-frequency dual-polarized antenna using interleaved slot arrays. Subscripts *c* and *x* on feed line labels refer to frequency band of that feed line.

The antenna bandwidth is determined by the required system-range resolution and look angle. For the next generation of instruments, bandwidths of between 50 to 100 MHz will be required. Fortunately, application characteristics demand the wider bandwidths at higher frequencies and this results in a fractional bandwidth of approximately 5% being generally acceptable, for any frequency. It should be pointed out that the bandwidth is typically defined at the 1.5:1 voltage standing wave ratio (VSWR) level (with the most significant contributions to the impedance mismatch being radiating element impedance bandwidth and external feed network mismatch). However, printed antennas, which are in many ways the most attractive candidates for DFDP applications, have inherently narrow-band characteristics. Therefore, it is very challenging to define an SAR system with bandwidth performance larger than 3–4% to be compatible with a printed DFDP antenna.

Polarization purity in a dual-polarized system is another important performance parameter. The main-lobe region has demanding polarization purity requirements, typically requiring the cross-polar level to be 25 dB below the copolar peak in the main-beam region and 20 dB below the copolar peak outside the main-beam region.

Elevation and azimuth beamwidths are determined by the antenna aperture size and the amplitude and phase excitations of the individual elements. Usually, a number of shaped beams are required in SAR antenna systems (often referred to as modes of operation). In azimuth the beam is usually fixed and broadened only very slightly, whereas in elevation, a highly shaped beam with a beam broadening factor up to

four is typically required. Typically, the beam is scanned in elevation, not exceeding 20° from the boresight position. Elevation sidelobes of the SAR antenna must be reduced to minimize range ambiguities. Normally, due to ambiguity suppression constraints, the most demanding requirement for beam shaping is at the highest steered angle.

Antenna gain is determined by the aperture size and dictated in turn by image resolution requirements. For a given aperture size and interelement separation, the antenna gain is optimized by selecting radiating elements with higher directivity and by reducing the loss. Antenna gain variation over frequency and temperature range is expected due to frequency-dependent element phase errors, VSWR degradation, element gain variations, mutual coupling, and other factors. From the SAR system point of view, it is important to maintain the antenna gain within each band at a certain minimum level. In general, this level is determined as a part of the system specification.

### III. DFDP ANTENNA CONCEPT ANALYSIS

A dual-frequency array can be conceived in one of two fundamental ways: using dual-frequency elements to cover both bands simultaneously or using interleaved single-frequency radiating elements for each band. Feed networks must also be integrated within the same aperture. For each of these methods, a number of concepts for specific implementation were evaluated. Since low cost, weight, and ease of manufacturing were primary considerations, only printed antenna elements were considered. Thus, using either microstrip patches, printed dipoles, or printed slots, a number of DFDP antenna concepts using either dual-frequency elements or single-frequency elements were considered.

For the present design, an array using dual-frequency elements requires elements that operate simultaneously at *C*- and *X*-band frequencies. Such elements include dual-frequency stacked patches [3], patches with “windows,” patches with grounding pins [5], notched patches [6], and dichroic patches [7]. Because of the approximately 2:1 frequency ratio, element spacing in the array is dictated by the requirement to avoid grating lobes at *X*-band, so that element spacing will be on the order of  $\lambda/2$  at *X*-band. This leads to an unnecessary increase in the number of elements at *C*-band, and a larger associated feed network. In addition, if the elements are resonant at *C*-band and the substrate dielectric constant is relatively low (preferable for good bandwidth), the size of the element may be large enough to preclude such close spacing (at least without strong mutual coupling effects) and/or crowding of the feed network. Alternatively, dual-frequency elements could be spaced for  $\lambda/2$  spacing at *C*-band, with single-frequency *X*-band elements interspersed between. Either of these methods is awkward for single-polarized arrays and probably unworkable for dual-polarized arrays.

For these reasons, it was determined that the use of dual-frequency elements was not the best choice for DFDP array applications. Other potential problems with specific dual-frequency elements include poor cross-pol performance (stacked patches, dichroic patches), too small of a ratio between the two frequencies (patches with grounding pins,

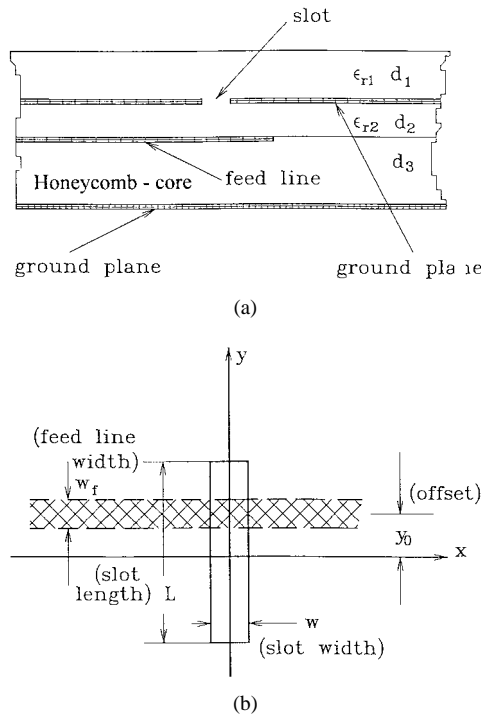


Fig. 2. (a) Cross-section of substrate geometry for slot array. (b) Plan view of slot antenna and feed-line geometry.

notched patches), and complicated feeding requirements (patches with windows). Coupling within a dual-frequency structures often results in distorted element patterns and poor isolation between bands.

We next discuss several possible array architectures using two interlaced *C*- and *X*-band arrays of dual-polarized single-frequency elements.

#### A. X-Band Printed Dipoles (Slots)/C-Band Printed Dipoles (Slots)

In Fig. 1 the concept for an interlaced array that employs either slots or printed dipoles is shown. Each element may be considered to be single frequency with a single polarization. As can be seen, elements of both types are fed with microstrip lines that run under the element. In the case of the slot, a single dielectric layer is required. For the printed dipole, two dielectric layers are required since the microstrip line is run on the lower layer with the dipoles printed on the upper layer. Since slots and dipoles take up less space than patches, it is expected that some benefit in terms of layout space for the signal distribution network (SDN) will be realized.

Note that it is possible to put the SDN for the two polarizations on different levels but orthogonal to each other so that they cross. In this layout, three dielectric layers are used, i.e., for the horizontal polarization (HP) SDN, the vertical polarization (VP) SDN, and the dipole elements. Coupling between the feed lines should be low (e.g.,  $-40$  dB) and, therefore, SDN design will be simplified.

An advantage of the slot array is that its SDN is hidden behind the ground plane where the slots are located and will, therefore, not contribute to spurious radiation. A disadvantage is that since a slot is bidirectional, a reflector ground plane

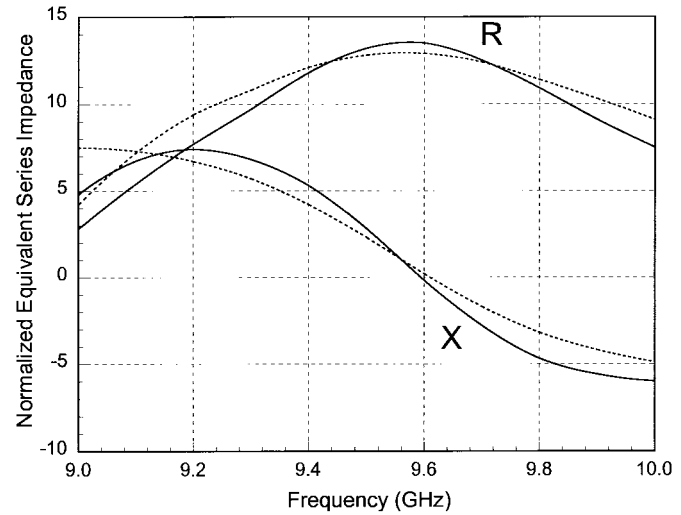


Fig. 3. Equivalent series impedance of a microstrip-fed slot element versus frequency normalized to  $50 \Omega$ . — slot length = 0.926 cm, width = 0.1 cm; — slot length = 0.935 cm, width = 0.20 cm; other parameters as given in Section IV.

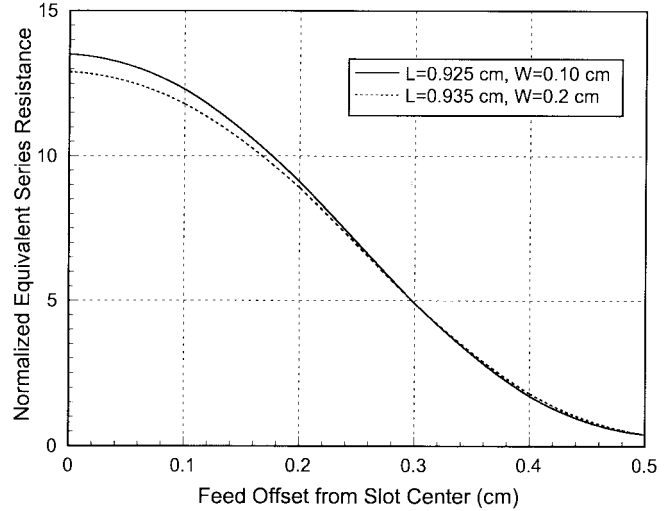


Fig. 4. Equivalent series impedance of a microstrip-fed slot antenna versus feed line offset  $y_0$  normalized to  $50 \Omega$ . Antenna parameters as given in Section IV.

must be placed at a distance of about  $\lambda/4$  behind the slot in order to direct the radiation in one direction only. This may result in potential problems due to waveguide modes, especially when scanning. The printed dipole array does not have the difficulty with bidirectionality of the slot array, since the dipole is already over a ground plane. However, the SDN will not be shielded and will contribute to cross-pol. In addition, two dielectric layers are required.

#### B. X-Band Patches/C-Band Patches

This architecture uses microstrip patches for both the *X*-band and *C*-band arrays. In order to make more room for the SDN and the patches themselves, one of the design alternatives is to increase the dielectric constant of the substrate. This will have the effect of making the size and the bandwidth of the printed elements smaller. If a substrate with a dielectric

constant of six is used rather than 2.3, then patch size may be reduced by about a factor of 1.5. Major disadvantages of this approach are that radiation efficiency decreases as the dielectric constant increases, impedance bandwidth is small, and mutual coupling effects are stronger due to increased surface wave energy.

### C. X-Band Slots/C-Band Patches

Slots and patches may be combined in an DFDP array. Such a configuration is shown in Fig. 5, where the *C*-band and *X*-band arrays are shown separately. The *C*-band patch array uses a microstrip SDN printed on the upper dielectric layer coplanar with the patches. Slots are printed in the ground plane of the *C*-band array and are fed with a microstrip SDN printed on a dielectric layer behind the ground plane. Since slots are bidirectional, a ground plane must be placed at about  $\lambda/4$  behind the SDN. The exact spacing is determined by the dielectric constant and thickness of the feed network substrate. A major advantage of this configuration is that the *X*-band and *C*-band SDN's can be separated, thus easing congestion for the dual-feed networks. In addition, the *X*-band SDN is isolated by the ground plane below the *C*-band array and will not radiate in the forward direction.

All of the above concepts were studied and evaluated against each other. As a result of this study it was concluded that the *C*-band patch/*X*-band slot concept had the greatest merit and this array design is now discussed in detail.

## IV. ANALYSIS AND DESIGN OF RADIATING ELEMENTS

In this section, we discuss the design details for the two types of radiating elements selected for the DFDP array. The section emphasizes printed slot design, since microstrip patch design data is more readily available [3]–[6].

### A. Slot Element

The substrate configuration for the array antenna has been chosen with regard to the construction of printed slot and patch elements and their associated feed networks, and is shown in cross section Fig. 2(a). The *C*-band patches and associated feed networks will be mounted on the top side of the top dielectric substrate while the slots are cut in the ground plane that separates the top and bottom dielectric layers. The feed networks for the slot elements are printed on the bottom side of the bottom substrate, as shown in planar view in Fig. 2(b). The table below lists the parameters of the substrate geometry:

top substrate dielectric constant	$\epsilon_{r1} = 2.94$
top substrate thickness	$d_1 = 1.78$ mm
bottom substrate dielectric constant	$\epsilon_{r2} = 2.94$
bottom substrate thickness	$d_2 = 0.762$ mm
ground plane spacing	$d_3 = 6.51$ mm
feed line impedance	$Z_0 = 50 \Omega$
feed line width	$w_f = 1.94$ mm.

The reflector ground plane at the bottom of the array is positioned so that the total electrical spacing between the two

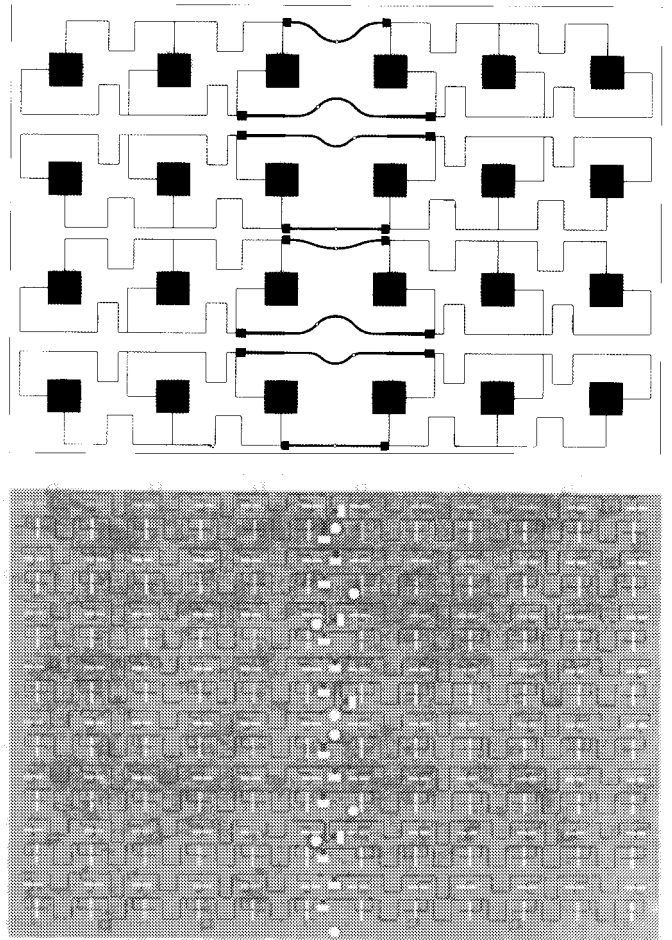


Fig. 5. Dual-frequency dual-polarized antenna using *C*-band patches and *X*-band slots. The *C*-band patch array layer overlays the *X*-band slot layer.

ground planes is  $\lambda/4$  at 9.6 GHz. The bottom substrate has an electrical thickness of  $15^\circ$ , while the 6.51-mm air space has a thickness of  $75^\circ$ . In practice this air space may be filled with foam. Because the main beam of the array is broadside (not scanned in azimuth) and the array elements are driven in phase, the possibility of deleterious parallel plate waveguide modes being excited between the ground planes is eliminated [8].

The slot element described above was analyzed using a general purpose full-wave moment-method solution that completely accounts for the dielectric layers and ground planes [9]. The theory of this solution has been previously described in the literature and has been tested for a variety of multilayer slot and dipole antennas with good results [9]. Calculated equivalent slot impedance as seen by the feed line is plotted versus frequency in Fig. 4, for two sets of slot dimensions. Note that this data is normalized to the feed-line impedance of  $50 \Omega$ . The first slot element has a length of  $L = 9.25$  mm and a width of  $W = 1$  mm and the second slot element has a length of  $L = 9.35$  mm and a width of  $W = 2$  mm. Both slots resonate at 9.6 GHz; the narrow slot has a resonant resistance of about  $675 \Omega$ , while the wider slot has a resonant resistance of about  $645 \Omega$ . These impedances are fairly high, but this is desirable for a series or resonant type of feed network where a number of elements effectively add in parallel. Wider slots typically lead to lower impedances, but as results show, the

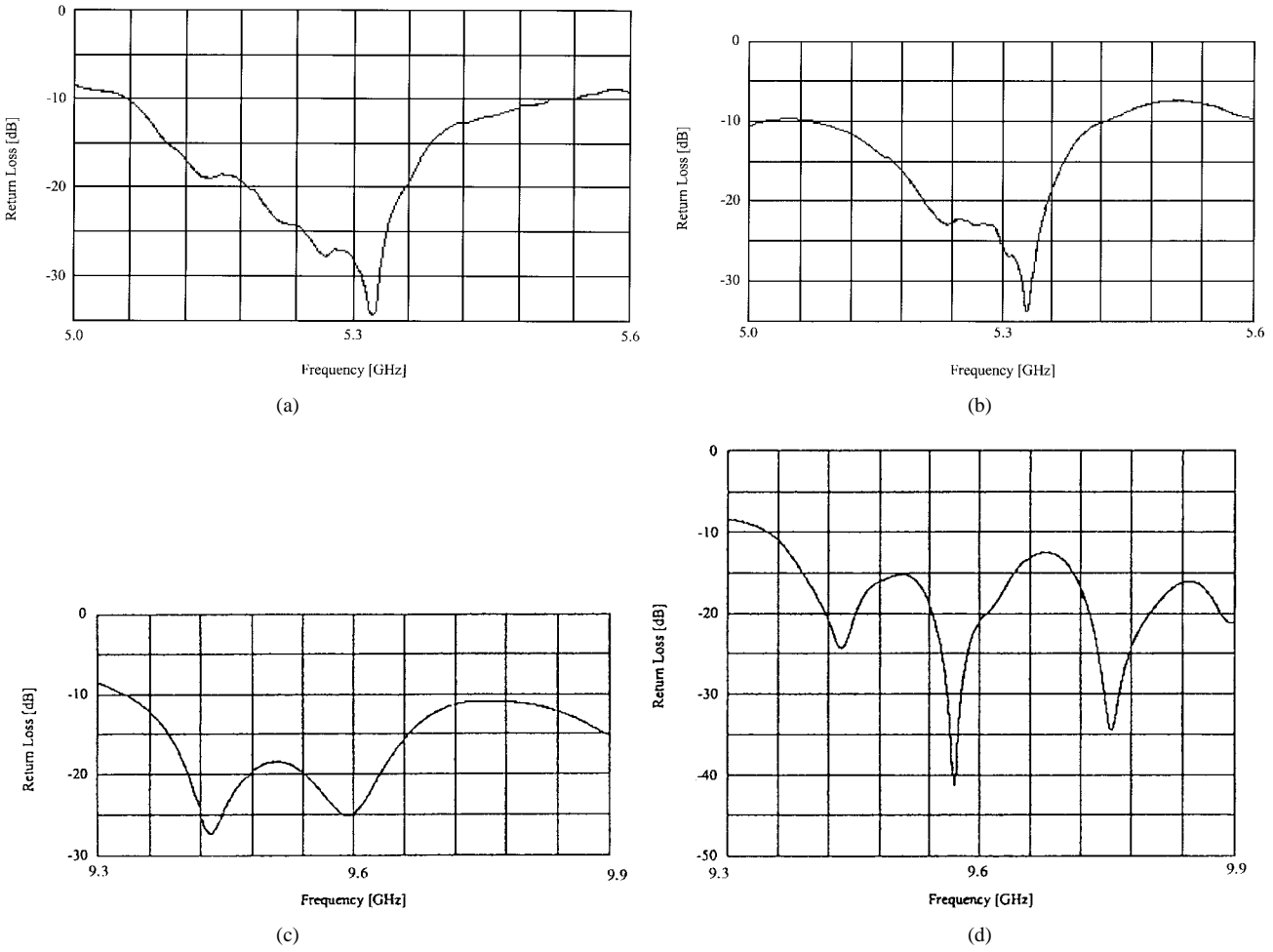


Fig. 6. (a) Measured return loss of the VP C-band subarray. (b) Measured return loss of the HP C-band subarray. (c) Measured return loss of the VP X-band subarray. (d) Measured return loss of the HP X-band subarray.

decrease is not substantial. In addition, wider slots will lead to higher cross-pol levels and decrease the space available for the cross-polarized elements and feed. The half-power bandwidth of both slot elements is in excess of 8%, which is much better than the performance requirements.

The data in Fig. 3 is for a feed line centered with the slot, while Fig. 4 shows the effect of a feed line offset from the center of the slot. It is seen that the (normalized) resonant resistance drops monotonically as the feed line is moved toward the edge of the slot. The resonant frequency does not change significantly as the feed line is moved.

### B. Patch Element

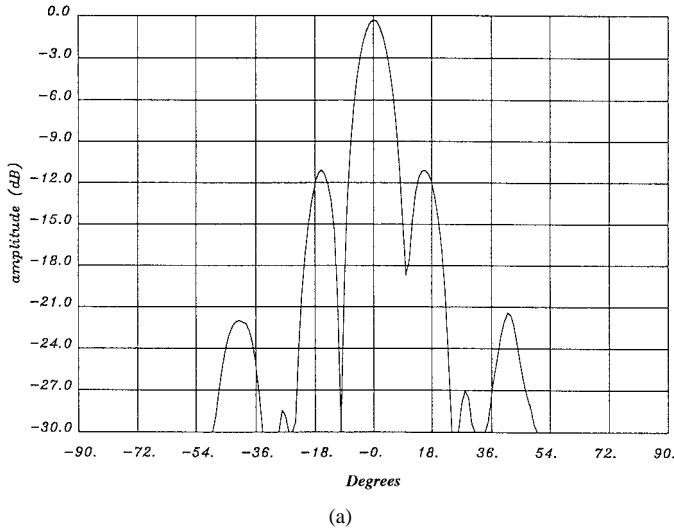
The patch element was designed to resonate at 5.3 GHz over a 2% (VSWR < 1.5) bandwidth. The substrate material was selected as a result of a tradeoff between bandwidth and cross-polar isolation performance. Substrates with higher dielectric constant are favored for lower cross-polar radiation [10], but at the same time they reduce the element-radiation efficiency and impedance bandwidth. For a compromise between these parameters, a substrate material with  $\epsilon_r = 2.94$  (Rogers Duroid 6002) was chosen. The substrate thickness was selected as a result of a tradeoff between bandwidth, surface wave energy, and feed network spurious radiation. Because the band-

width requirement was not very demanding, a relatively thin substrate ( $d/\lambda_0 = 0.03$ ) was selected in order to obtain good cross-pol and sidelobe performance in an array environment. The patch element was fed from a coplanar microstrip line with a  $150\Omega$  characteristic impedance. The patch dimensions were determined in two steps. The approximate dimensions were initially obtained from a simple cavity model and then the exact dimensions were obtained from a thru-reflect-line (TRL)-calibrated reflection coefficient measurement. The final patches were square with 15.39-mm sides. The measured complex  $S_{11}$  parameter was subsequently used in the optimization of the C-band subarray feed network.

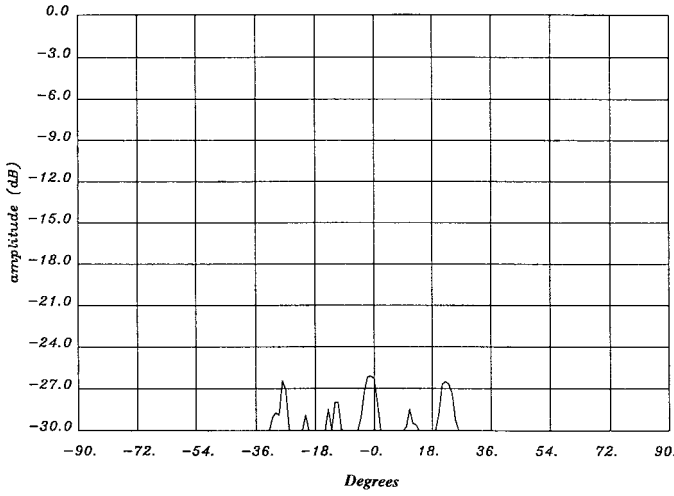
## V. ARRAY DESIGN

### A. Layout Optimization

In order to minimize or eliminate grating lobes for a given scanning range, element spacing must be between  $\lambda/2$  and  $\lambda$ . As the current requirement has no azimuth scan, the element spacing in the orthogonal direction may be close to  $\lambda$ . There is a 1.81 : 1 ratio between the center frequencies in this design. However, to avoid physical interference between the elements of the high- and low-frequency arrays and to maximize the spacing between elements of parallel polarization, the C-band



(a)



(b)

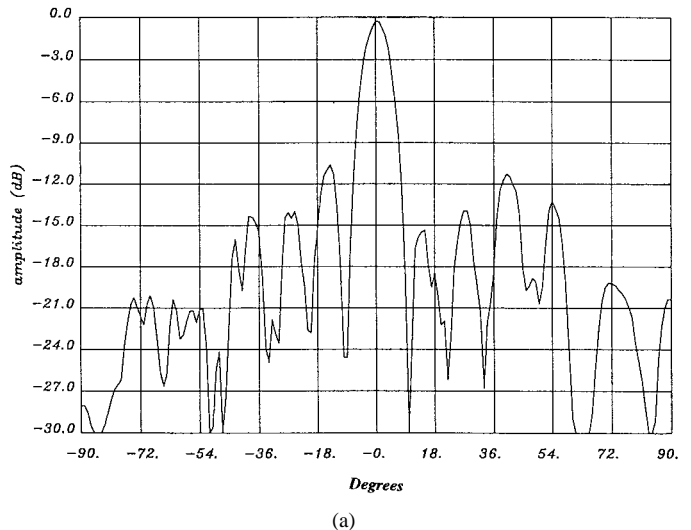
Fig. 7. (a) Measured azimuth copolar pattern of the VP C-band array. (b) Measured azimuth crosspolar pattern of the VP C-band array.

and  $X$ -band element spacings are chosen as a 2:1 ratio. Fig. 5 shows the final layout of the DFDP antenna with the above requirements in mind. Note that some  $C$ -band input feedlines are curved in order to avoid blocking the  $X$ -band feed points below. Final layout parameters were as follows:

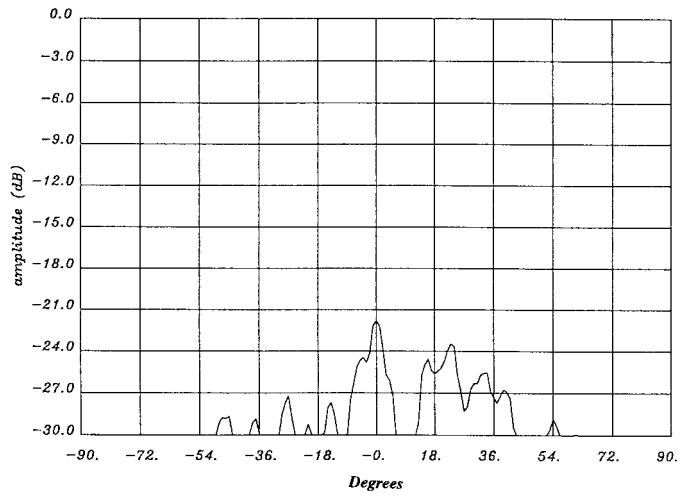
Vertical $X$ -band slot spacing:	$0.80\lambda$
Horizontal $X$ -band slot spacing:	$0.78\lambda$
Vertical $C$ -band patch spacing:	$0.89\lambda$
Horizontal $C$ -band patch spacing:	$0.89\lambda$ .

### B. Feed Network Design

The radiating elements of both bands are organized into linear subarrays. This condition is essential because of the scanning requirements and facilitates RF power distribution. For the development model described here each VP and HP  $C$ -band subarray contained six elements. The number of elements in each  $X$ -band subarray is 12. For simplicity of design and for testing flexibility, the subarrays are interfaced with an external RF power distribution network via a  $50\Omega$  coaxial connector.



(a)



(b)

Fig. 8. (a) Measured azimuth copolar pattern of the HP C-band array. (b) Measured azimuth crosspolar pattern of the HP C-band array.

Parasitic coupling between feed lines was minimized using full-wave simulations of the layout.

A series/parallel standing wave feed network was selected as a best compromise for bandwidth and minimum phase-error performance for the available feed substrate area. In addition, the feed network was designed to uniformly excite the elements in both amplitude and phase. The feed design approach was identical for  $C$ -band and  $X$ -band subarrays. It was based on the use of the measured  $S$ -parameters of a single element as an electrical model of a one-port device in the circuit optimization performed with the linear circuit simulator "touchstone." Circuit discontinuities such as T-junctions and bends were modeled using full-wave analysis and represented in the model in terms of their  $S$ -parameters. Some matching features like step discontinuities and open-ended stubs were optimized using "touchstone" models. The optimization strategy was aiming at a minimum of 20-dB return loss over the bandwidth.

The  $100\Omega$  input lines of each subarray were connected in parallel to a  $50\Omega$  SMA coaxial connector. During the

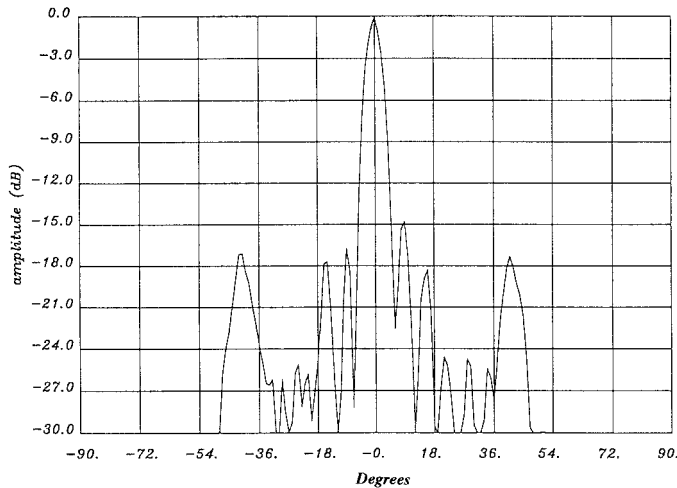


Fig. 9. Measured azimuth copolar pattern of the VP X-band array.

design phase the VSWR of *C*-band and *X*-band transitions were optimized using the finite-element software HFSS from Hewlett Packard.

## VI. DFDP SAR ANTENNA PROOF OF CONCEPT DESCRIPTION

The proof of concept (POC) antenna consists of four tiles (i.e., panels). Two of them (stacked vertically) are electrically active, while the other two are passive. Each tile consists of four rows of six-element *C*-band subarrays and eight rows of 12-element *X*-band subarrays. Each tile was laminated to form a sandwich of Teflon (PTFE) layers, Nomex honeycomb spacer, and thin aluminum ground plane. SMA connectors for each subarray were assembled to the ground plane. The antenna was fed from an RF source using 1:8 (*C*-band) and 1:16 (*X*-band) microstrip power splitters.

## VII. MEASURED RESULTS

Initial testing evaluated the return-loss performance of each *C*-band and *X*-band subarray. Typical frequency responses of the antenna subarrays are shown in Fig. 6(a)–(d). Four to 5% 1.5:1 VSWR bandwidth was typically measured for the *C*-band subarrays, whereas 2–3% bandwidth was achieved for the *X*-band subarrays. The reduced bandwidth of the *X*-band slot arrays was due to the relatively narrow bandwidth of its series feed network, which was somewhat longer electrically than the *C*-band feed network. The antenna patterns were measured in a planar near-field test range at three frequencies for each array. Both copolar and cross-polar patterns were obtained by Fourier transformation of the near field data. Representative antenna patterns are presented in Figs. 7–10.

The measured patterns indicate that radiation from single aperture using dual-polarized arrays operating at two distant and not harmonically related frequencies is feasible. The interference between arrays as reflected in the main-lobe distortions is minimal. Sidelobe levels in azimuth were typically measured at -12 dB. Such increased sidelobe level is not unexpected, mainly due to spurious radiation from the microstrip feed network. In a full-size SAR antenna, the sidelobe level can be controlled by an external azimuth and elevation feed network.

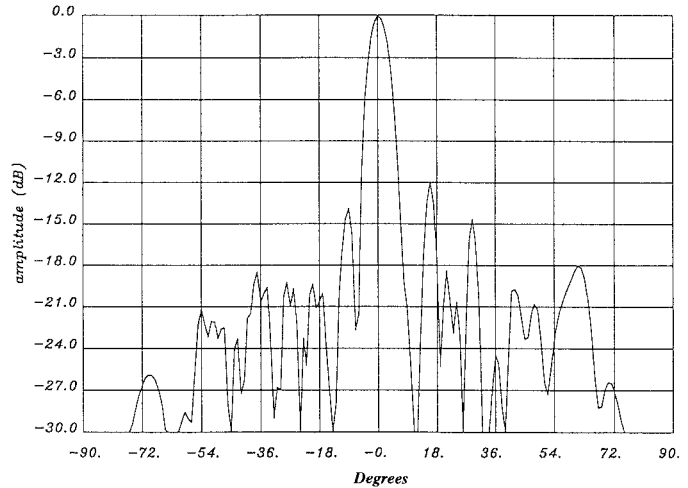


Fig. 10. Measured azimuth copolar pattern of the HP X-band array.

The sidelobe pattern indicates that some excitation errors exist within subarrays. It was found that the lamination process slightly alters the effective dielectric constant of the substrates, hence, the electric path between subarray elements differs from a multiple of a wavelength. The cross-polar level for the *C*-band antenna was quite low (less than -21 dB) over the full-view angle. For the *X*-band array, the cross-polar radiation was slightly higher (about -18 dB), probably due to difficulties in optimizing the layout of the microstrip-to-coax interfaces.

## VIII. CONCLUSIONS

Various methods of implementing a shared-aperture DFDP array antenna were considered with a *C*-band patch and *X*-band slot array being chosen as optimum for the present requirements. Layout considerations for the two interlaced arrays and their associated feed networks were addressed to realize a practical design. A dual-frequency (*C*- and *X*-band), dual-linear polarized SAR array antenna prototype was developed and demonstrated. The principal goal of the development—to demonstrate the viability of the concept with an acceptable level of interference between four separate arrays within a single radiating aperture—has been accomplished. Test results were shown to be good with good correlation between measured and predicted results, validating the design approach used.

Although further development is necessary before the concept discussed can be used in a fielded system, the work described here has demonstrated that the application of a dual-frequency dual-polarization SAR antenna within a single aperture is a feasible approach to meeting user requirements in future SAR spacecraft.

## ACKNOWLEDGMENT

The authors would like to thank D. Warne and A. Rhodes of Spar Aerospace for their support and inspiring technical discussions.

## REFERENCES

- [1] R. L. Jordan, B. L. Huneycutt, and M. Werner, "The SIR-C/X-SAR synthetic aperture radar system," *Proc. IEEE*, vol. 79, pp. 827-837, June 1991.
- [2] G. L. Rait, "SIR-C L-band dual-polarization synthetic aperture radar antennas," in *Proc. Microwave Instrumentat. Remote Sensing Earth (MIRSE) Conf.*, Orlando, FL, Apr. 1993, vol. 1935, pp. 84-94.
- [3] R. Bancroft, "Accurate design of dual-band patch antennas," *Microwaves RF*, Sept. 1988.
- [4] S. S. Zhong and Y. T. Lo, "Single element rectangular microstrip antenna for dual frequency operation," *Electron. Lett.*, vol. 19, no. 8, pp. 298-300, Apr. 1983.
- [5] H. Nakano and K. Vichien, "Dual frequency square patch antenna with rectangular notch," *Electron. Lett.*, vol. 25, no. 16, pp. 1067-1068, Aug. 1989.
- [6] J. R. James and G. Andrasic, "Superimposed dichroic microstrip antenna arrays," *Proc. Inst. Elect. Eng.*, vol. 135, pt. H, no. 5, pp. 304-312, Oct. 1988.
- [7] R. J. Mailloux, "On the use of metallized cavities in printed slot arrays with dielectric substrates," *IEEE Trans. Antennas Propagat.*, vol. AP-35, pp. 477-487, May 1987.
- [8] N. K. Das and D. M. Pozar, "Multiport scattering analysis of general multilayered printed antennas fed by multiple feed ports—Part I: Theory; Part II: Applications," *IEEE Trans. Antennas Propagat.*, vol. 40, pp. 469-491, May 1992.
- [9] R. C. Hansen, "Cross-polarization of microstrip patch antennas," *IEEE Trans. Antennas Propagat. Soc.* vol. APS-35, no. 6, pp. 731-732, June 1987.

**Ralph Pokuls** received the M.Eng. and Ph.D. degrees from McGill University, Montreal, Quebec, Canada, in 1984 and 1988, respectively.

From 1988 to 1990, he taught courses in electromagnetics at McGill University and was engaged in research on reflector antenna synthesis. Since 1990 he has been employed at Spar Aerospace, Montreal, Quebec, as a Specialist Antenna Engineer. He has been engaged in research work on reflector antennas, dielectric loaded horns, microstrip antennas, reflectarrays and active arrays.



**Jaroslaw Uher** (M'88) received the Dr.Ing (Ph.D.E.E.) degree in electrical engineering from the University of Bremen, Germany, in 1987.

From 1988 to 1990, he was a Postdoctoral Fellow and Research Engineer at the University of Ottawa, Canada, where he was working on numerical methods for electromagnetic modeling of microwave and millimeter-wave components. In 1990, he joined the Antenna Group at Spar Aerospace Ltd., Spar Space Systems, Ste-Anne-de-Bellevue, Que, Canada, where he is currently a

Specialist in Spacecraft Antenna Engineering. At Spar, he was involved in the development of advanced SAR antennas for remote sensing application. He holds a patent for a dual-polarized dual-frequency SAR array antenna. He is currently involved in the development of active arrays for communication satellite systems. He is a coauthor of *Waveguide Components for Antenna Feed Systems, Theory and CAD* (Norwood, MA: Artech House, 1993).

**D. M. Pozar** (S'74-M'80-SM'88-F'90), for photograph and biography, see p. 1625 of the November 1997 issue of this TRANSACTIONS.